Langmuir–Shäfer Transfer of Fullerenes and Porphyrins: Formation, Deposition, and Application of Versatile Films

Sabrina Conoci,[g] Dirk M. Guldi,[b] Sara Nardis,[c] Roberto Paolesse,[c] Konstantinos Kordatos,[d] Maurizio Prato,[d] Giampaolo Ricciardi,[e] M. Graça H. Vicente,[f] Israel Zilbermann,[b] and Ludovico Valli*[a]

Dedicated to the memory of our friend and colleague Professor Luigi Pasimeni, who actively and enthusiastically promoted the collaboration among the authors.

Abstract: Thin films consisting of a fulleropyrrolidine derivative **1** and a novel water-soluble porphyrin **2** were prepared by the Langmuir–Shäfer (LS, horizontal lifting) method. In particular, a solution of **1** in chloroform and dimethyl sulfoxide was spread on the water surface, while porphyrin **2** (bearing peripheral anionic groups) was dissolved into the aqueous subphase. To the best of our knowledge, such a versatile method of film fabrication for fullerene/porphyrin mixed composite films has never been used before. Evidence of the effective interactions between the two moieties at the air–water interface was obtained from the analysis of the floating layers by means of surface pressure versus area per molecule Langmuir curves, Brewster angle microscopy and UV-visible reflection spectroscopy. The characterisation of the LS films by UV-visible spectroscopy reveals that the two constituents behave as discrete and weakly interacting π systems. The use of polarised light suggests the existence of a preferential direction of the macrocyclic rings with an edge-on arrangement with respect to the substrate surface. Finally, photoaction spectra were recorded from films deposited by only one horizontal lifting onto indium–tin–oxide (ITO) electrodes and the observed photocurrent increased notably with increasing transfer surface pressure.

Keywords: fullerenes · monolayers · porphyrins · thin films

Introduction

The molecularly governed construction of nanostructured films has been dominated by the ingenious Langmuir–Blodgett (LB) technique for about 70 years. Recently electrostatically driven assembly methods have gained attention as a very promising techniques in the field of template-assisted assembly: oppositely charged materials are used in order to fabricate high-quality coatings whose thickness is controlled at the nanometer level.[1] The most substantial advantage of both techniques is the accurately controlled layer thickness, thus implying that the macroscopic characteristics of the molecular film can be governed by the size of the microscopic arrangement of the different units.

The energy- and electron-accepting ability of [60]fullerene and its derivatives have made a notable impact in the field

[a] Prof. L. Valli
Dipartimento di Ingegneria dell'Innovazione
Università degli Studi di Lecce
Via Prov.le Lecce-Monteroni, 73100 Lecce (Italy)
Fax: (+39) 0832-297525
E-mail: ludovico.valli@unile.it

[b] Prof. D. M. Guldi, Dr. I. Zilbermann
Institute for Physical Chemistry
Friedrich-Alexander-Universität Erlangen-Nürnberg
91058 Erlangen (Germany)

[c] Dr. S. Nardis, Prof. R. Paolesse
Dipartimento di Scienze e Tecnologie Chimiche
Via della Ricerca Scientifica, Università di Tor Vergata
00133 Roma (Italy)

[d] Dr. K. Kordatos, Prof. M. Prato
Dipartimento di Scienze Farmaceutiche
Università degli Studi di Trieste
Piazzale Europa, 1, 34127 Trieste (Italy)

[e] Prof. G. Ricciardi
Dipartimento di Chimica, Università della Basilicata
Via N. Sauro, 85, 85100 Potenza (Italy)

[f] Dr. M. G. H. Vicente
Department of Chemistry, Lousiana State University
Baton Rouge, LA 70803 (USA)

[g] Dr. S. Conoci
Sioptics & post Silicon Technologies
Corporate R&D STMicroelectronics
Stradale Primosole, 50, 95121 Catania (Italy)

 DOI: 10.1002/chem.200400520

of the photoinduced charge-separation processes. Moreover, the observation that C_{60} is a powerful electron acceptor—susceptible of receiving up to six electrons[2]—has rendered the use of [60]fullerene almost unique in conjunction with electron donors. Thus, several distinct donor–acceptor structures incorporating [60]fullerene and its derivatives have been satisfactorily prepared and investigated during the last decade.[3] C_{60} manifests, however, comparatively weak absorbance in the visible portion of the electromagnetic spectrum; however, when it is associated with an electron-donating chromophore that exhibits adequate absorption features, the resulting dyads typically represent important models for artificial photosynthetics. Macrocyclic compounds, such as porphyrins[4] or phthalocyanines,[5] are exceptionally well suited as photoexcited electron donors. Once the electron is transferred from the porphyrin to the fullerene moiety, the generated π-radical cation is usually delocalised among the different macrocyclic electron donors, as already demonstrated for chemical sensors based on these macrocycles.[6]

Among the techniques used to fabricate photoactive films based on C_{60} derivatives and porphyrins or phthalocyanines, there are the simple solvent-casting,[7] Langmuir–Blodgett,[8,9] thermal evaporation,[10] layer-by-layer,[11] self-assembly,[12] spin-coating[13] and vacuum deposition[14] methods.

It is known that [60]fullerene and most of its derivatives form condensed layers on the water surface,[15] mostly as a consequence of the strong cohesive energy of more than 30 kcal mol^{-1}.[16] This accounts for the existence of intense intermolecularly attractive π–π interactions and very stable van der Waals aggregates, even at the air–water interface. Concentration of the spreading solution, nature and volume of the spreading solvent, and compression rate are all fundamental parameters in determining the quality of the floating film of C_{60} derivatives.[17] Therefore, in our approach towards high-quality fullerene films, dilute spreading solutions (concentration less than 10^{-4} M) of the fullerene derivative, small volumes (always less than 50 μL) and very low speed of compression (4 cm^2 min^{-1}) have been used.

The fullerene derivative **1** and the water soluble porphyrin **2** have been prepared according to recently published synthetic protocols.[18,19]

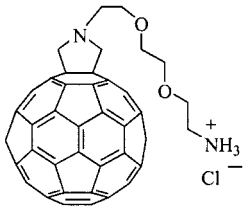

1

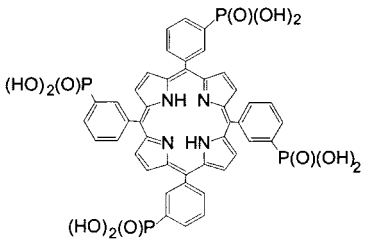

2

Results and Discussion

The Langmuir curves of **1** have been measured for both pure water and a subphase containing the water-soluble porphyrin **2** and are reported in Figure 1.

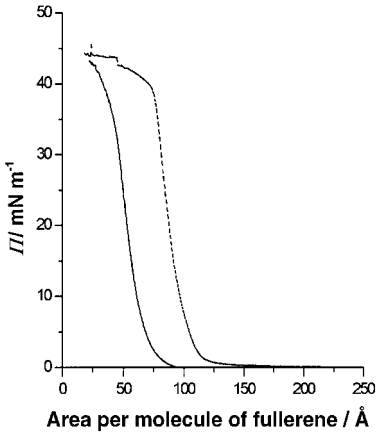

Figure 1. Langmuir curves for fullerene derivative **1** on a pure-water surface (solid line) and on a solution of porphyrin **2** (dotted line) at 25 °C. Spreading solution concentration: 10^{-4} M; solvent: mixture of chloroform and dimethylsulfoxide (see Experimental Section).

The two curves appear considerably different, thus providing first evidence of the effective interaction between the fullerene derivative **1** and the porphyrin **2** dissolved in the subphase. The presence of **2** causes a shift of the curve towards larger areas by more than 30 Å^2. In fact, the limiting areas (obtained by extrapolation to zero surface pressure of the steepest and linear portion of the Langmuir curves) for pure water and the porphyrin aqueous solution subphases are 66 and 100 Å^2 per fullerene molecule, respectively. This means that the presence of the $-NH_3^+$ termination in compound **1** is insufficient to render it adequately amphiphilic and to allow the generation of a real monolayer on the pure water surface. On the other hand, the dissolution in the subphase of **2** and the presence of its peripheral anionic groups induce an efficient electrostatic interaction, promoting the formation of a more homogeneous floating layer. Such interactions are energetically at least of the same order of magnitude as the strong, cohesive, intermolecular π–π interactions, namely, $\geq$30 kcal mol^{-1}.[16] In the following we gather further evidence in support of the effective influence of the water-soluble porphyrin **2** on the organisation of fullerene derivative **1** on the subphase surface.

Brewster angle microscopy (BAM) is a rather recent and powerful technique usually utilised to monitor directly the morphology of floating layers at the air–water interface.[20] In actual interfaces, the intensity of the reflected radiation is mainly determined by the interfacial characteristics and evidences a minimum at the Brewster angle. Both the thickness of the floating layers and the roughness at the interface are critical parameters that determine the BAM images. Since the BAM investigation was carried out during the compression of the floating layer, this method provided essential information about the presence of pure **1** aggregates on the water surface. For example, when pure **1** was spread on the subphase, the existence of large, three-dimensional aggregates floating onto the clean water surface was observed, even immediately after the spreading solvent evaporation. In Figure 2a, facets are clearly seen at low surface pressures (i.e., 0.1 mN m^{-1}) and low area densities (i.e., 93 Å^2). The large fullerene clusters contain porous voids, which corre-

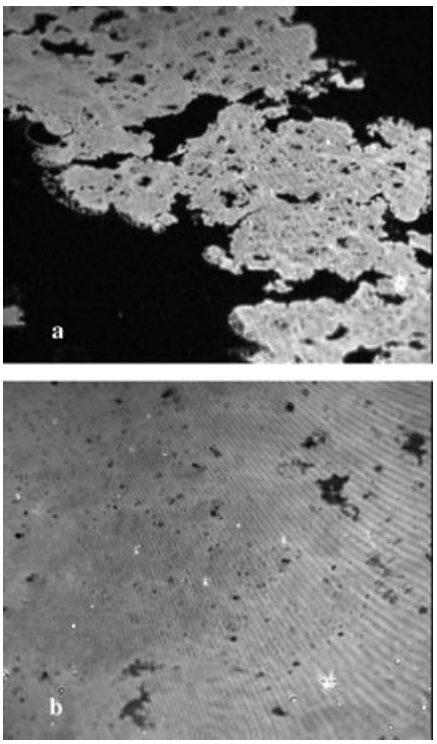

Figure 2. BAM images of pure fullerene derivative **1** at the air–water interface at a surface pressure of a) 0.1 mN m^{-1} and b) 5 mN m^{-1}. The field of view of the BAM instrument along the x axis is 430 μm.

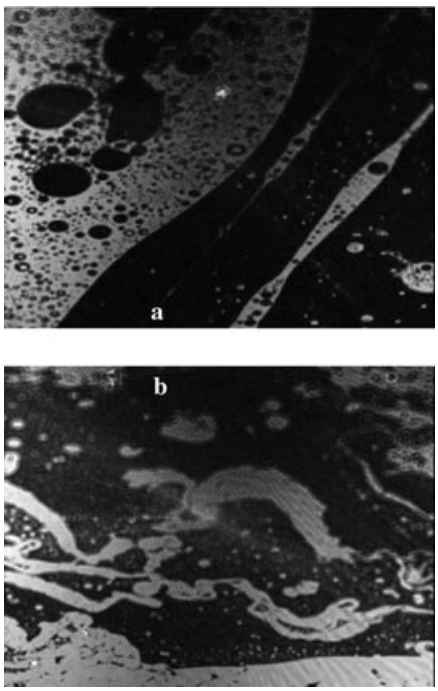

Figure 3. BAM images of fullerene derivative **1** at the air–water interface at a surface pressure of a) 0.1 mN m^{-1} and b) 5 mN m^{-1}. The water-soluble porphyrin **2** was dissolved in the aqueous subphase. The area of the BAM instrument along the x axis is 430 μm.

spond to pure water surfaces, with dimensions in the range 10–50 μm; the field of view of the BAM instrument is 430 μm along the x axis. Figure 2b confirms that at higher surface pressure (i.e., 5 mN m^{-1}) and an area per fullerene derivative of about 68 Å^2 such morphology becomes denser and denser and the voids containing water become progressively smaller and smaller.

Introduction of the water-soluble porphyrin **2** into the subphase gave rise to considerable and peculiar influence on the structure and morphology of the floating layer. The image in Figure 3a was taken at a surface pressure of 0.1 mN m^{-1}, which corresponds to an area per fullerene derivative of about 220 Å^2, and appears absolutely different from that reported in Figure 2a. The electrostatic interactions between cationic **1** and anionic **2** at the air–water interface have induced the generation of a more homogeneous and supposedly thinner floating film. The distinct and sharp edges and facets, as evidenced for **1** on the pure water subphase, have now disappeared and have been substituted by continuous and regular boundaries. In Figure 3b, which was taken at 5 mN m^{-1} (i.e., area per fullerene derivative of about 104 Å^2), the black subphase surface in Figure 2a has been replaced by a greyish region contiguous to brighter and thicker domains. The rationale is the coexistence of a monolayer of **1** and areas of fullerene–porphyrin aggregates.

The presence and active participation in interfacial phenomena of the porphyrin has also been corroborated by the reflection spectroscopy under normal incidence in the UV-visible range; these measurements were carried out directly on the floating film on the water surface.[21] This unconventional but powerful method is particularly suited for this purpose, since only chromophores that are located at the interface contribute to the enhanced reflection. In particular, the difference in reflectivity (ΔR) from the chromophore floating layer on the subphase and from the bare subphase surface was monitored as a function of wavelength. The corresponding reflection spectra of **1** on pure water surface at two different fixed surface pressures, namely, 0.1 and 5 mN m^{-1} after reaching equilibrium conditions (i.e., no variation in surface pressure and enhanced reflectivity), are shown in Figure 4. It is apparent that upon compression the reflection enhances, because the surface density grows while the profile remains constant. The increase in ΔR suggests that, after the initial aggregation subsequent to solution spreading, the self-organised and associated clusters are dragged on the water surface and coalesce, while consequently the surface density of the floating layer is enhanced. This spectral behaviour is also consistent with the pattern seen in the Langmuir curves, see above.

Upon introduction into the subphase of **2**, a new strong peak emerges, which corresponds to the Soret band of the porphyrin. Interestingly, this transition is even apparent at 0.1 mN m^{-1}, which provides further evidence that the fullerene/porphyrin interactions are active, even just after spreading the solutions. Because only those chromophores that are located at the air–liquid interface affect the enhanced reflection,[21] these spectra also substantiate the accumulation of **2** at the interface by means of electrostatic interactions with the oppositely charged **1**. In the spectrum taken at 5 mN m^{-1}, a loss of signal intensity of the fullerene deriva-

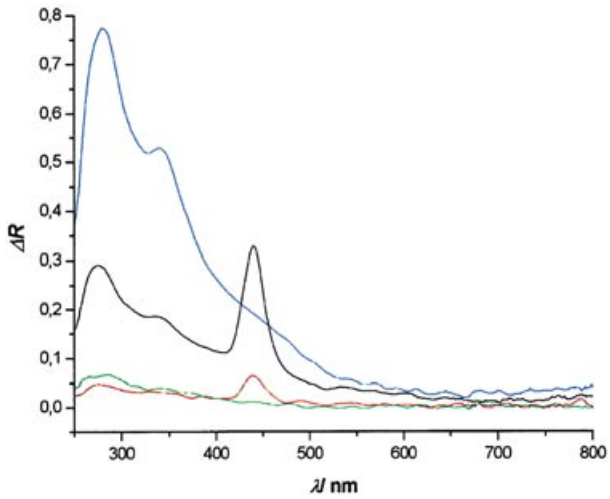

Figure 4. Absolute reflection spectra of **1** on a pure-water surface at surface pressures of 0.1 mN m^{-1} (green) and 5 mN m^{-1} (blue) and on an aqueous solution of **2** at surface pressures of 0.1 mN m^{-1} (red) and 5 mN m^{-1} (black).

tive is noted when **2** is present in the subphase. This is yet another piece of evidence in support of the strong interactions between **1** and **2**. In fact, a plausible rationale is that **2** intercalates between the molecules of **1**; this intercalation would lead to fewer chromophores per surface unit.

The deposition of such layers onto different substrates (i.e., glass, quartz, silicon, indium–tin–oxide (ITO)) was carried out by the horizontal lifting (Langmuir–Schäfer, LS) method. Films obtained by up to 40 horizontal liftings were deposited, though even thicker films could be transferred.

An inspection of the absorption spectrum of a 30 layer LS film reveals the following features. Firstly, the UV region is dominated by optical absorptions of the C_{60} subunits, while the porphyrin absorptions are very weak in this region. The characteristic and very intense π–π* absorption of C_{60} is clearly discernible in the spectrum of the LS film at 262 nm, a value very close to that observed in the solution spectrum.

Secondly, the intense Soret band and the weaker $Q_x(0.0)$, $Q_x(1.0)$, $Q_y(0.0)$ and $Q_y(1.0)$ bands of the **2** system are also discernible in the near-UV region, at 428 nm, and in the visible region, at 644, 586, 545 and 517 nm, respectively. The Soret band shows a bathochromic shift (ca. 14 nm) with respect to the solution spectrum of **2**; however, a comparable bathochromic shift has been observed for solution spectra of **2** over the period of a few hours after dissolution of the porphyrin; this behaviour could be attributed to the formation of porphyrinic dimeric species, mediated by hydrogen-bonding interactions between the peripheral phosphonic groups of adjacent subunits. At variance indeed with the previously studied 4-phosphonatophenyl isomer, which was found to give extended aggregates,[22] the porphyrin **2**, due to the geometric position of the peripheral substituents that prevents the formation of extended aggregates, tends to form dimeric species.[23] In view of the significant photoconduction response of the system (vide infra) it cannot be excluded, however, that a non-negligible contribution to this bathochromic shift may arise, in the quasi solid state, from effective interactions between the π systems of **1** and **2**.[24,25]

Thirdly, a rather weak absorption due to bending deformations of the O–H groups belonging to interstitial water and to the porphyrin peripheral functions, and of the C–H groups present in the fullerene substituent, extends in the near-IR up to 2500 nm.

The films are also investigated with polarised light, with the light polarisation plane parallel or perpendicular to the incidence plane of radiation at an incidence angle $I = 0°$ of the light beam with respect to the plane normal to the lifting direction. The main absorptions of **1** and **2** show a small, but significant dependence on the direction of the electric field vector, see Figure 5. These dependencies suggest that the

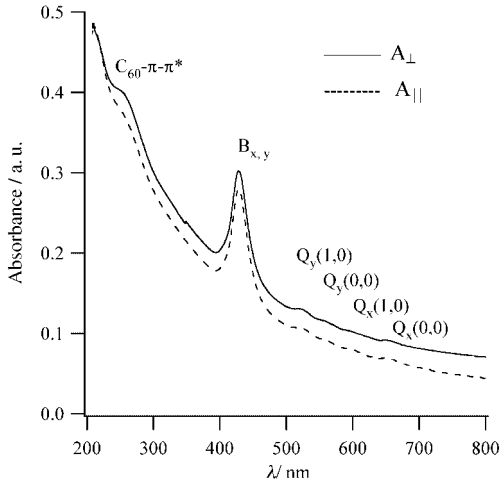

Figure 5. Electronic spectrum in polarised light of the Langmuir–Shäfer film (30 layers) fabricated with **1** and **2**: electric field vector parallel to the incidence plane (dashed line); electric field vector perpendicular to the incidence plane (solid line).

films exhibit a significant molecular order. Whereas safe predictions on the ordering of the fullerene subunits can hardly be made on the basis of these observed spectral changes, analysis of the dichroic ratios measured for the porphyrin absorptions leads us to think that the macrocyclic rings are preferentially edge-on-oriented with respect to the surface (i.e., quartz).

Next, we investigated the structure of ITO/(**1**+**2**), in which the monolayers were produced at the air–water interface and transferred onto the ITO electrodes with the LS method at several surface pressures (i.e., 2, 5, 15, 20, and 25 mN m^{-1}); photocurrent experiments were performed, that is, the response of light illumination on the generation of electrical energy was measured. Exact experimental conditions were 0.1 M NaH_2PO_4, 1 mM ascorbic acid and nitrogen. Replacing 0.1 M NaH_2PO_4 with 0.1 M NaCl, while leaving 1 mM ascorbic acid and nitrogen, led to a fivefold drop in the photocurrent.

Saturation of the aqueous electrolyte solution (0.1 M NaH_2PO_4, without ascorbic acid) with oxygen led to a threefold intensification of the photocurrent. Considering that the reduction potential of $C_{60}/C_{60}\int^-$ couple in fulleropyrrolidines ($E_{1/2} = -1.05$ V versus Fc/Fc$^+$) relative to that of the $O_2/O_2^{\bullet-}$ couple ($E_{1/2} = -0.91$ V versus Fc/Fc$^+$; pH 7) an elec-

tron transfer from the primary electron acceptor (i.e., $C_{60}^{\bullet-}$) to molecular oxygen is thermodynamically possible.[26] In fact, several photolytical and radiolytical studies, all conducted in aqueous media, have shown that $O_2^{\bullet-}$ is generated upon electron transfer from $C_{60}^{\bullet-}$.[27] Once oxygen is reduced to superoxide radical anion, it acts as a very mobile electron carrier to transport the negative charge to the electron-collecting ITO electrode.

After the preparation, the photoaction spectra of the modified ITO electrodes were recorded and a representative photoaction spectrum of an ITO/(**1**+**2**) electrode is reported in Figure 6. An excellent match is noted with the absorption

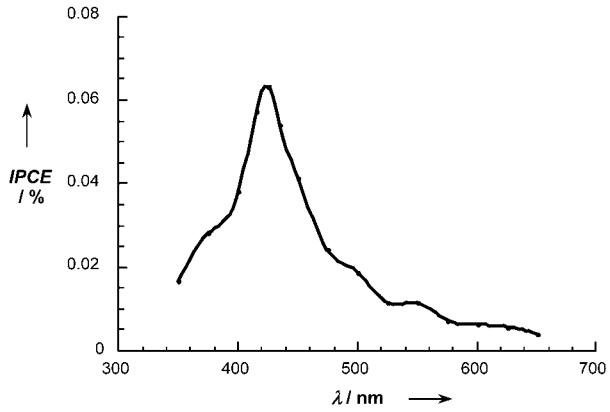

Figure 6. Photoaction spectrum of a modified ITO-electrode bearing a mixed **1**/**2** coverage (deposited at a surface pressure of 25 mN m^{-1}) under deoxygenated conditions (i.e., no bias voltage is applied).

spectrum seen in the reflection experiments. To be precise, the porphyrin's Soret and also Q-band features are noticeable. The features of C_{60}, on the other hand, are masked by the ITO absorption at wavelengths <350 nm. With the photoaction spectrum in hand, we were able to confirm the origin of the photocurrents, namely, that porphyrin is the photoactive species.

Mechanistically, a picture evolves that is sketched in Figure 7. An important factor is that the above-described deposition of **1**/**2** places the electron acceptor (i.e., **1**) in close proximity to the ITO electrodes, while the electron-donor/chromophore system (i.e., **2**) is located at the aqueous interface.

Upon the initial photoexcitation event of **2**, a thermodynamically driven electron transfer to **1** occurs. (For recent reviews on fullerene-containing donor–acceptor ensembles and fullerene anions see reference [28].) Electron injection from reduced **1** into the conduction band of ITO (i.e., -0.25 V versus SCE)[29] and sacrificial electron transfer from ascorbate to oxidised **2** help to reinstate the ground state of **1**/**2**.

Interestingly, the photocurrents increased notably with increasing surface pressure, which corresponds to a closer packing of the dyad molecules. This observation can be rationalised on the grounds of higher absorption cross sections at higher surface pressures (see the section on reflection spectroscopy). The incident photon to current conversion efficiency (IPCE) values were 0.022 (2 mN m^{-1}), 0.038 (5 mN m^{-1}), 0.048 (15 mN m^{-1}), 0.061 (20 mN m^{-1}) and 0.064 (25 mN m^{-1}).

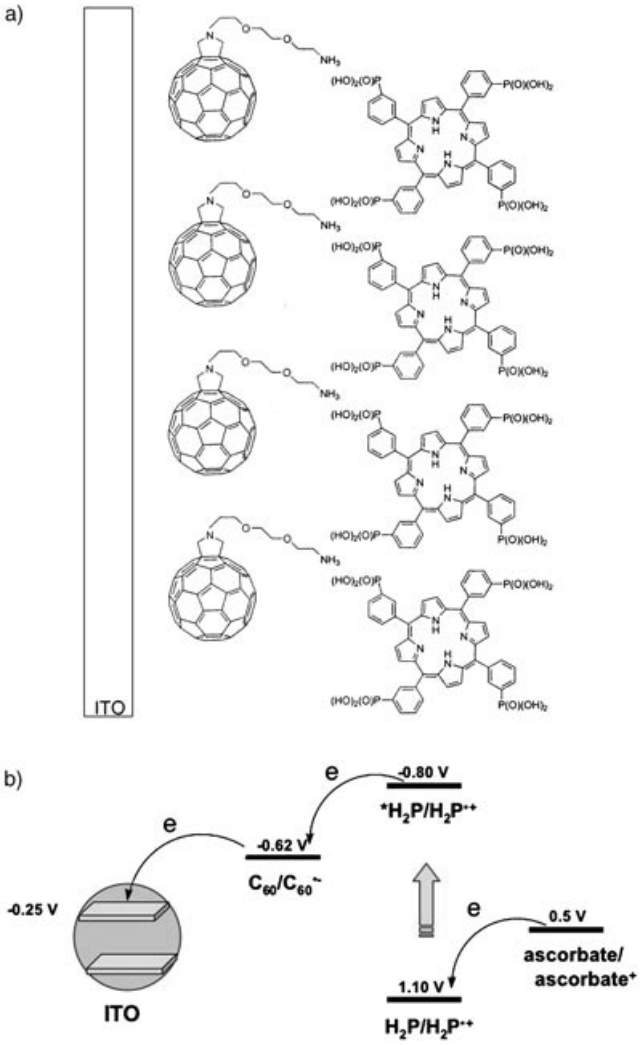

Figure 7. a) Organisation of **1**/**2** onto ITO electrodes. b) Schematic representation of electron-transfer events in modified ITO-electrodes bearing a mixed **1**/**2** coverage.

Relative to bare ITO electrodes and ITO electrodes that just carry a fullerene monolayer, for which we measured IPCE values of less than 0.001 and 0.01 %,[30] respectively, we consider our current finding to be an appreciable improvement. Interestingly, films transferred at the highest surface pressure (i.e., 25 mN m^{-1}) reveal IPCEs that are similar to those of ZnP–C_{60},[31] NiP–C_{60},[32] and H_2P–C_{60} systems[33] that were assembled through electrostatic interactions.

To probe the stability of the photocurrents, a modified ITO electrode was illuminated over several time intervals. Only a 337 nm filter was employed to cut-off the wavelength region that would correspond to the illumination of the ITO electrode itself. Importantly, the response to ON/OFF cycling (i.e., turning the light source on and off) was prompt and reproducible. Over the monitored time window of 60 s a moderate decrease in current of less than 5 % was noted.

Atomic force microscopy (AFM) inspection of one layer of both pure **1** and the mixed **1**/**2** systems deposited at

25 mN m^{-1} onto hydrophobised silicon substrates is reported in Figure 8. In the case of the film of pure **1** (Figure 8, top), the surface appears covered by a network of nanorods, with hole-like defects, much larger than those observed for the mixed **1/2** layer (vide infra). The lateral dimensions of these rodlike objects range between 20–60 nm, whereas the height is 2–7 nm. The related root mean square roughness (RMS) is about 1.8 nm. The **1/2** mixed layer (Figure 8, bottom) shows a quite different morphology if compared with that of pure **1**. It exhibits the appearance of homogeneously dispersed nanorods, which are tens of nanometers (10–20 nm) in diameter and 1–2 nm high. The measured RMS is approximately 0.9 nm (note that the hydrophobic silicon substrate shows values of RMS of about 0.2 nm). All these results agree with recent literature data concerning similar fullerene derivatives.[34]

Insights into the morphology of the multilayers obtained by this mixed method have been gained by the top view AFM images related to films obtained after five horizontal liftings for both pure **1** and mixed **1/2** films (Figure 9). In both cases, the surfaces show rodlike-shaped nanostructures with lateral dimensions essentially similar to those observed for the monolayers. However, the molecular organisation is quite different for the two systems. In the case of pure **1** coatings (Figure 9, top), the film is much more rough than the monolayer, with a consequent increase of RMS value up to about 2.2 nm. In contrast, the layers of the **1/2** system (Figure 9, bottom) appear more homogeneous, densely packed and flat. Accordingly, the related RMS is now about 1.3 nm.

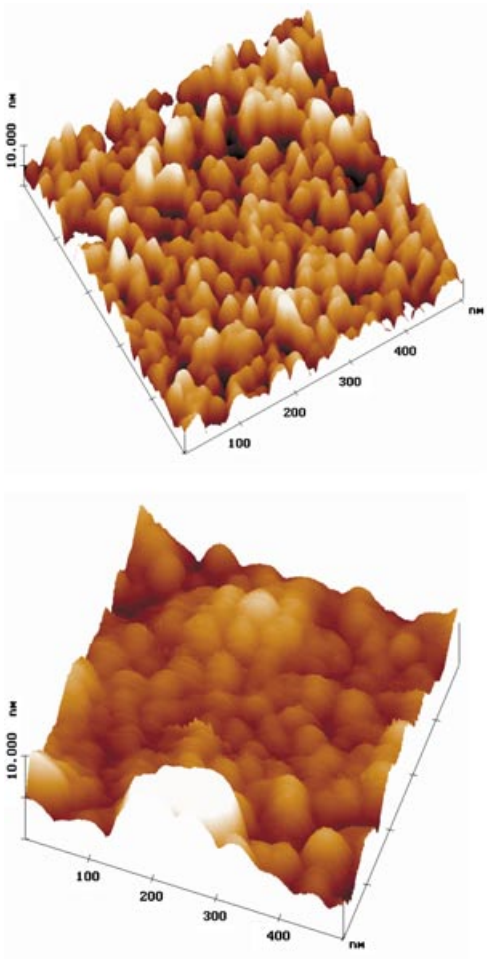

Figure 9. Atomic force microscopy three-dimensional images of five layers of pure **1** (top) and of a mixture of **1/2** (bottom) deposited on hydrophobic silicon substrates.

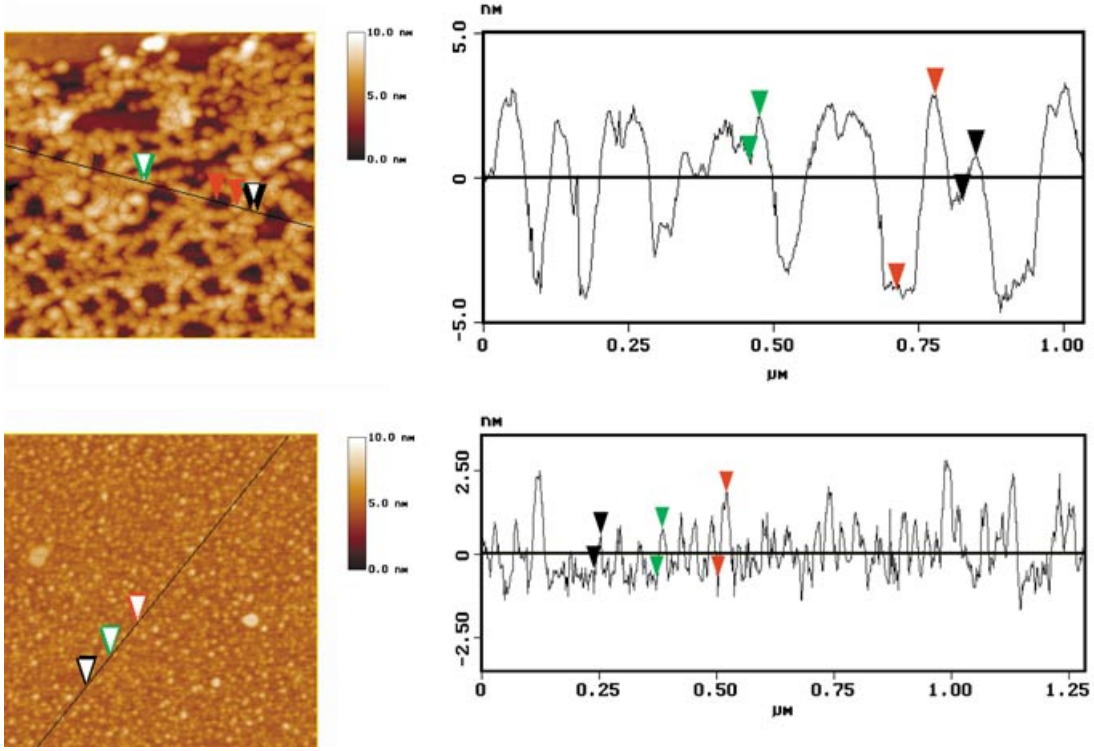

Figure 8. Atomic force microscopy images of a monolayer of pure **1** (top) and of a mixture of **1/2** (bottom) deposited on hydrophobic silicon substrates.

It is worth noting that the above AFM data are in good agreement with the BAM analysis, which showed larger homogeneity of the floating films of the **1**/**2** composite.

In conclusion, we have constructed mixed composite thin films consisting of a cationic fulleropyrrolidine derivative (**1**) and an anionic porphyrin derivative (**2**) dissolved in the subphase. We have fabricated high-quality, robust and photoactive films by making use of the horizontal lifting method and electrostatic interactions. To the best of our knowledge we have for the first time organised such moieties through this unique and powerful procedure. Moreover, such a combination of donor (i.e., **2**) and acceptor moieties (i.e., **1**) held in close proximity by electrostatic interactions leads to photocurrent generations that exhibited a meaningful efficiency increase with increasing transfer pressures. All these considerations suggest the utilisation of the described method of deposition as a new effective technique for the fabrication of functioning devices that contain fullerene and macrocyclic derivatives as active species for photocurrent generation. Our research is currently proceeding with new, charged fullerene and porphyric moieties in order to change the cation-to-anion charge ratio and to check how such parameters reflect on molecular organisation and vary the film response to light illumination.

Experimental Section

Synthesis: The fullerene derivative **1** and the water soluble porphyrin **2** were prepared according to recently published synthetic protocols.[18,19]

Langmuir experiments: Chloroform (Fluka, HPLC grade) and dimethyl sulfoxide (Fluka, GC grade) were used in making up the spreading solution: fullerene derivative **1** (1.71 mg, 1×10^{-3} mmol) was completely dissolved in a few drops of dimethyl sulfoxide and then chloroform was added up to give a total volume of the solution of 10 mL. Langmuir experiments were carried out on a KSV5000 System3 apparatus. Ultrapure water (resistivity larger than 18 MΩ cm) from a Milli-Q system was used as the subphase (pH ;5.9). It was thermostated at 20 °C by a Haake GH-D8 apparatus. A 200 μL aliquot of the spreading solution was spread onto the subphase. After solvent evaporation, the floating film was compressed at a speed of 5 Å^2 per molecule per minute. During the depositions, the transfer surface pressure was fixed at different values (2, 5, 10, 15, 20, and 25 mN m^{-1}). Glass, quartz and silicon substrates were all rendered hydrophobic before deposition by storing overnight in a dessicator in contact with vapour of 1,1,1,6,6,6-hexamethydisilazane. The transfer of all substrates was performed by the horizontal lifting method (Langmuir–Schäfer technique).

Reflection spectroscopy and Brewster angle microscopy: Reflection spectroscopy and Brewster angle microscopy (BAM) analysis were carried out by using an NIMA 601BAM apparatus. Again, a compression speed of 5 Å^2 per molecule per minute was utilised. The reflection data (ΔR) were obtained on an NFT RefSpec instrument. They were acquired under normal incidence of radiation according to the description given in reference [35] and correspond to the difference between the reflectivities of the floating film–liquid interface and the clean air–liquid interface. BAM measurements were obtained on an NFT BAM2plus system with a lateral resolution of 2 μm.

UV-visible and near-IR spectroscopy: Electronic solution spectra in 0.1 cm path length quartz cells in the region 200–2500 nm were performed on a UV-vis-NIR 05E Cary spectrophotometer equipped with a polarised spectroscopy set-up. A Glan–Taylor polariser was set between the lamp and sample to obtain desired polarised UV-visible irradiation.

Photoelectrochemical measurements: Photoelectrochemical measurements were carried out in a three-armed cell that had provision to insert a working (ITO), counter (Pt gauze) and reference electrodes (Ag/AgCl, when bias voltage was applied). The electrolyte was either 0.1 M NaH_2PO_4 (pH 7) or 0.1 M NaCl (pH 7) and N_2 or O_2 was bubbled into the solution for 10–15 minutes prior to photoelectrochemical measurements. Photocurrent measurements were carried out on a Keithley model 617 programmable electrometer immediately after illumination. A collimated light beam from a 150 Xenon lamp was used for UV illumination. When white light was used, a 375 nm cut filter was used. When recording a photoaction spectrum, a Bausch and Lomb high-intensity grating monochromator was introduced into the path of the excitation beam for selecting the required wavelengths. The incident photon to current conversion efficiency (IPCE), defined as the number of electrons collected per incident photon, was evaluated from short circuit photocurrent measurements at different wavelengths versus the photocurrent measured using a photodiode of the type PIN UV 100 (UDT Sensors Inc.).

Atomic force microscopy: The atomic force microscopy (AFM) images were acquired in air by using a Digital 3100 microscope in the tapping mode. Commercially available tapping etched silicon probes (Digital) with a pyramidal shape tip that has a nominal curvature of 10 nm and a nominal internal angle of 35° were used.

Acknowledgement

The authors wish to thank Luigi Dimo for his technical support during Langmuir experiments. This work was carried out with partial support from the EU (RTN networks "WONDERFULL" and "CASSIUSCLAYS"), MIUR (PRIN 2002, prot. 2002032171 and 2002033817), FISR (D.M. 16/10/20), Project SAIA (2003), the Universities of Lecce and Trieste, and the Office of Basic Energy Sciences of the US Department of Energy. This is document NDRL-4562 from the Notre Dame Radiation Laboratory. I.Z. acknowledges his sabbatical leave from the Nuclear Research Centre Negev, Beer Sheva (Israel).

[1] *Multilayer Thin Films, Sequential Assembly of NanoComposite Materials* (Eds.: G. Decher and J. B. Schlenoff), Wiley-VCH, Weinheim, **2003**.
[2] L. Echegoyen, L. E. Echegoyen, *Acc. Chem. Res.* **1998**, *31*, 593–601.
[3] a) N. Armaroli in *Photoinduced Energy Transfer Processes in Functionalized Fullerenes in Fullerenes: From Synthesis to Optoelectronic Properties* (Eds: D. M. Guldi, N. Martin), Kluwer, Dordrecht, **2002**, pp. 137–162, and references therein; b) P. J. Bracher, D. I. Schuster in *Electron Transfer in Functionalized Fullerenes in Fullerenes: From Synthesis to Optoelectronic Properties* (Eds: D. M. Guldi, N. Martin), Kluwer, Dordrecht, **2002**, pp. 163–212, and references therein.
[4] a) P. A. Liddell, J. P. Sumida, A. N. Macphrson, L. Noss, G. R. Seely, K. N. Clark, A. L. Moore, T. A. Moore, D. Gust, *Photochem. Photobiol.* **1994**, *60*, 537–541; b) N. Ohta, S. Mikami, Y. Iwaki, M. Tsushima, H. Imahori, K. Tamaki, Y. Sakata, S. Fukuzumi, *Chem. Phys. Lett.* **2003**, *368*, 230–235; c) N. V. Tkachenko, V. Vehmanen, J.-P. Nikkanen, H. Imahori, S. Fukuzumi, H. Lemmetyinen, *Chem. Phys. Lett.* **2002**, *366*, 245–252; d) D. M. Guldi, C. Luo, D. Koktysh, N. A. Kotov, T. Da Ros, S. Bosi, M. Prato, *Nano Lett.* **2002**, *2*, 775–780.
[5] a) J. Chen, J. Zhang, Y. Shen, X. Liu, *Proc. SPIE-Int. Soc. Opt. Eng.* **2000**, *4086*, 749–752; b) D. Tanaka, M. Rikukawa, K. Sanui, N. Ogata, *Synth. Met.* **1999**, *102*, 1492–1493; c) M. Rikukawa, S. Furumi, K. Sanui, N. Ogata, *Synth. Met.* **1997**, *86*, 2281–2282.
[6] A. Tepore, A. Serra, D. P. Arnold, D. Manno, G. Micocci, A. Genga, L. Valli, *Langmuir* **2001**, *17*, 8139–8144.
[7] V. Vehmanen, N. V. Tkachenko, H. Imahori, S. Fukuzumi, H. Lemmetyinen, *Spectrochim. Acta A* **2001**, *57*, 2229–2244.
[8] A. S. Alekseev, N. V. Tkachenko, A. Y. Tauber, P. H. Hynninen, R. Osterbacka, H. Stubb, H. Lemmetyinen, *Chem. Phys.* **2002**, *275*, 243–251.
[9] R. Marczak, K. Noworyta, W. Kutner, G. Suresh, F. D'Souza, *Proc. Electrochem. Soc.* **2003**, *13*, 47–54.
[10] D. Godovsky, L. Chen, L. Pettersson, O. Inganäs, M. R. Andersson, J. C. Hummelen, *Adv. Mater. Opt. Electron.* **2000**, *10*, 47–54.

[11] D. M. Guldi, F. Pellarini, M. Prato, C. Granito, L. Troisi, *Nano Lett.* **2002**, *2*, 965–968.
[12] A. Ikeda, T. Hatano, S. Shinkai, T. Akiyama, S. Yamada, *J. Am. Chem. Soc.* **2001**, *123*, 4855–4856.
[13] N. Ohta, S. Mikami, Y. Iwaki, M. Tsushima, H. Imahori, K. Tamaki, Y. Sakata, S. Fukuzumi, *Chem. Phys. Lett.* **2003**, *368*, 230–235.
[14] K. Takahashi, K. Etoh, Y. Tsuda, T. Yamaguchi, T. Komura, S. Ito, K. Murata, *J. Electroanal. Chem.* **1997**, *426*, 85–90.
[15] L. Valli, D. M. Guldi, *Langmuir–Blodgett Films of C_{60} and C_{60}-Materials in Fullerenes: From Synthesis to Optpelectronic Properties* (Eds: D. M. Guldi, N. Martin), Kluwer, Dordrecht, **2002**, pp. 327–385, and references therein.
[16] a) F. Cardullo, F. Diederich, L. Echegoyen, T. Habicher, N. Jayaraman, R. M. Leblanc, J. F. Stoddart, S. Wang, *Langmuir* **1998**, *14*, 1955–1959; b) C. Pan, M. P. Sampson, Y. Chai, R. H. Hauge, J. L. Margrave, *J. Phys. Chem.* **1991**, *95*, 2944–2946; c) X. Shi, W. B. Caldwell, K. Chen, C. A. Mirkin, *J. Am. Chem. Soc.* **1994**, *116*, 11598–11599.
[17] L. Leo, G. Mele, G. Rosso, L. Valli, G. Vasapollo, D. M. Guldi, G. Mascolo, *Langmuir* **2000**, *16*, 4599–4606.
[18] K. Kordatos, T. Da Ros, S. Bosi, E. Vazquez, M. Bergamin, C. Cusan, F. Pellarini, V. Tomberli, B. Baiti, D. Pantarotto, V. Georgakilas, G. Spalluto, M. Prato, *J. Org. Chem.* **2001**, *66*, 4915–4920.
[19] F. Odobel, E. Blart, M. Lagre′e, M. Villieras, H. Boujtita, N. El Murr, S. Caramoric, C. A. Bignozzi, *J. Mater. Chem.* **2003**, *13*, 502–510.
[20] R. Castillo, S. Ramos, J. Ruiz-Garcia, *Physica A* **1997**, *236*, 105–113.
[21] H. Kuhn, D. Möbius, *Monolayer assemblies, in Physical Methods of Chemistry, Vol. IXB, Investigations of Surfaces and Interfaces—Part B*, (Eds.: B. W. Rossiter, R. C. Baetzold), Wiley Interscience, New York, **1993**, pp. 375–542.
[22] M. De Napoli, S. Nardis, R. Paolesse, M. G. H. Vicente, R. Laceri, R. Purrello, *J. Am. Chem. Soc.* **2004**, *126*, 5934–5935.
[23] R. Purrello, R. Laceri, M. De Napoli, S. Nardis, R. Paolesse, M. G. H. Vicente, unpublished results.
[24] A. P. H. J. Schenning, D. H. W. Hubert, M. C. Feiters, R. J. M. Nolte, *Langmuir* **1996**, *12*, 1572–1577.
[25] J. M. Kroon, R. B. M. Koehorst, M. van Dijk, G. M. Sanders, E. J. R. Sudhölter, *J. Mater. Chem.* **1997**, *7*, 615–624.
[26] a) Y. Yamakoshi, S. Sueyoshi, K. Fukuhara, N. Miyata, T. Masumizu, M. Kohno, *J. Am. Chem. Soc.* **1998**, *120*, 12363–12364; b) V. Ohlendorf, A. Willnow, H. Hungerbühler, K. D. Asmus, D. M. Guldi, *J. Chem. Soc. Chem. Commun.* **1995**, 759–760.
[27] a) Y. Yamakoshi, N.; Umezawa, A. Ryu, K. Arakane, N. Miyata, Y. Goda, T. Masumizu, T. Nagano, *J. Am. Chem. Soc.* **2003**, *125*, 12803–12809; b) N. Miyata, Y. Yamakoshi, *Free Radical Biol. Med.* **1999**, *27*, 291; c) Y. Yamakoshi, S. Sueyoshi, K. Fukuhara, N. Miyata, *J. Am. Chem. Soc.* **1998**, *120*, 12363–12364; d) R. V. Bensasson, M. Brettreich, J. Frederiksen, H. Gottinger, A. Hirsch, E. J. Land, S. Leach, D. J. McGarvey, H. Schonberger, *Free Radical Biol. Med.* **2000**, *29*, 26–33; e) D. M. Guldi, *J. Phys. Chem. B*, **2000**, *104*, 1483–1489.
[28] a) H. Imahori, Y. Sakata, *Adv. Mater.* **1997**, *9*, 537–546; b) M. Prato, *J. Mater. Chem.* **1997**, *7*, 1097–1109; c) N. Martin, L. Sanchez, B. Illescas, I. Perez, *Chem. Rev.* **1998**, *98*, 2527–2547; d) H. Imahori, Y. Sakata, *Eur. J. Org. Chem.* **1999**, 2445–2457; e) F. Diederich, M. Gomez-Lopez, *Chem. Soc. Rev.* **1999**, *28*, 263–277; f) D. M. Guldi, *Chem. Commun.* **2000**, 321–327; g) D. M. Guldi, M. Prato, *Acc. Chem. Res.* **2000**, *33*, 695–703; h) C. A. Reed, R. D. Bolskar, *Chem. Rev.* **2000**, *100*, 1075–1119; i) D. Gust, T. A. Moore, A. L. Moore, *J. Photochem. Photobiol. B* **2000**, *58*, 63–71; j) D. Gust, T. A. Moore, A. L. Moore, *Acc. Chem. Res.* **2001**, *34*, 40–48; k) D. M. Guldi, N. Martin, *J. Mater. Chem.* **2002**, *12*, 1978–1992; l) D. M. Guldi, *Chem. Soc. Rev.* **2002**, *31*, 22–36.
[29] F. Fromherz, W. Arden, *J. Am. Chem. Soc.* **1980**, *102*, 6211–6218.
[30] D. M. Guldi, I. Zilbermann, G. Anderson, A. Li, D. Balbinot, N. Jux, M. Hatzimarinaki, A. Hirsch, M. Prato, *Chem. Commun.* **2004**, 726–727.
[31] I. Zilbermann, G. A. Anderson, D. M. Guldi, H. Yamada, H. Imahori, S. Fukuzumi, *J. Porphyrins Phthalocyanines* **2003**, *7*, 357–364.
[32] D. M. Guldi, I. Zilbermann, G. A. Anderson, K. Kordatos, M. Prato, R. Tafuro, L. Valli, *J. Mater. Chem.* **2004**, *14*, 303–309.
[33] D. M. Guldi, I. Zilbermann, G. Anderson, A. Li, D. Balbinot, N. Jux, M. Hatzimarinaki, A. Hirsch, M. Prato, *Chem. Commun.* **2004**, 726.
[34] M. Mannsberger, A. Kukovecz, V. Georgakilas, J. Rechthaler, G. Allmeier, M. Prato, *XVII International Winterschool/Euroconference on Electronic Properties of Novel Materials*, (Ed.: H. Kuzmany) Kichberg, Tirol, **2003**.
[35] H. Grüniger, D. Möbius, H. Meyer, *J. Chem. Phys.* **1983**, *79*, 3701–3710.

Received: May 25, 2004
Published online: November 11, 2004

